Journal of proteome research

Article

pubs.acs.org/jpr

Identification of Novel miR-21 Target Proteins in Multiple Myeloma Cells by Quantitative Proteomics

Qian Xiong,[†,⊥] Qiu Zhong,[‡,⊥] Jia Zhang,[†,§] Mingkun Yang,[†] Chongyang Li,[†] Peng Zheng,[†] Li-Jun Bi,*[,§] and Feng Ge*[,†]

[†]Institute of Hydrobiology, Chinese Academy of Sciences, Wuhan, 430072, China

[‡]IBP-ARI Joint Center for Research on Tuberculosis, Antituberculosis Research Institute of Guangdong Province, Guangzhou 510630, China

[§]Key Laboratory of Non-coding RNA, Institute of Biophysics, Chinese Academy of Sciences, Beijing 100101, China

Supporting Information

ABSTRACT: Substantial evidence indicates that microRNA-21 (miR-21) is a key oncomiR in carcinogenesis and is significantly elevated in multiple myeloma (MM). In this study, we explored the role of miR-21 in human MM cells and searched for miR-21 targets. By knocking down the expression of endogenous miR-21 in U266 myeloma cells, we observed reduced growth, an arrested cell cycle, and increased apoptosis. To further understand its molecular mechanism in the pathogenesis of MM, we employed a SILAC (stable isotope labeling by amino acids in cell culture)-based quantitative proteomic strategy to systematically identify potential targets of miR-21. In total, we found that the expression of 178 proteins was up-regulated significantly by miR-21 inhibition, implying that they could be potential targets of miR-21. Among these, the protein inhibitor of activated STAT3 (PIAS3) was confirmed as a direct miR-21 target by Western blotting and reporter gene assays. We further demonstrated that miR-21 enhances the STAT3-dependent signal pathway by inhibiting the function of PIAS3 and that down-regulation of PIAS3 contributes to the oncogenic function of miR-21. This elucidation of the role of PIAS3 in the miR-21-STAT3 positive regulatory loop not only may shed light on the molecular basis of the biological effects of miR-21 observed in MM cells but also has direct implications for the development of novel anti-MM therapeutic strategies.

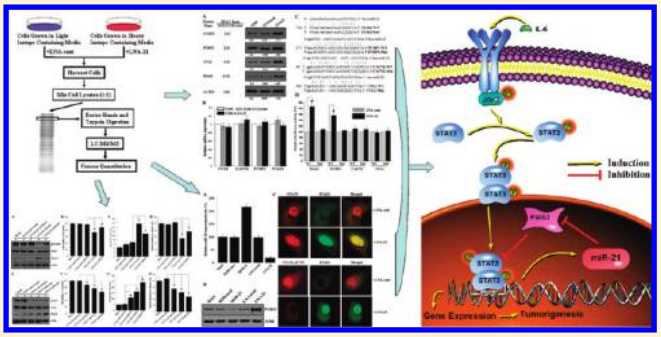

KEYWORDS: *microRNA-21 (miR-21), multiple myeloma (MM), stable isotope labeling by amino acids in cell culture (SILAC), signal transducer and activator of transcription 3 (STAT3), protein inhibitor of activated STAT3 (PIAS3)*

INTRODUCTION

Multiple myeloma (MM) is a clonal B-cell malignancy characterized by the accumulation of terminally differentiated, antibody-producing plasma cells in the bone marrow[1] and is the leading cause of death in hematologic malignancies.[2] Its incidence varies globally from 1 per 100000 people in China to about 4 per 100000 people in most developed countries.[1,2] Despite advances in understanding the molecular pathogenesis of MM and promising new therapies, MM remains incurable and the majority of patients eventually succumb to their cancer.[3] Current models assume that MM evolves through a multistep transformation process and accumulation of genetic and epigenetic alterations. Deregulation of hundreds of genes and multiple signaling pathways leads to MM pathogenesis and disease progression. As many of these genes and signaling pathways are regulated by microRNAs (miRNAs), miRNAs either as tumor suppressors or oncogenes play an important role in the progression and pathogenesis of MM.[4]

miRNAs are small, noncoding RNAs of 19−25 nucleotides in length found in diverse organisms.[5] miRNAs act as negative regulators of gene expression by binding to the 3′-untranslated region (UTR) of their target mRNAs with partial or full sequence complementarity, thereby leading to mRNA translational inhibition or degradation.[6] To date, 1424 human miRNAs have so far been identified (http://www.mirbase.org, miRBase v.17.0) and are predicted to regulate the expression of around 60% of all human protein-encoding genes.[7] By silencing various target mRNAs, miRNAs have key roles in diverse regulatory pathways, including control of development, cell differentiation, apoptosis, cell proliferation, and protein secretion.[8−11] Importantly, miRNAs have been reported to play crucial roles in the pathogenesis of MM.[12−14] miR-21 is an oncogenic miRNA that is overexpressed in MM cells[4] and

Received: June 1, 2011
Published: February 8, 2012

whose elevation significantly promotes survival of multiple myeloma.[15]

miR-21 is a unique miRNA in that it is overexpressed in the vast majority of cancer types analyzed so far[16] and has thus been recognized as an oncomiR.[17] Inhibition of miR-21 was shown to cause decreased cell growth *in vitro* and decreased tumor growth in a xenograft mouse model,[18] increased apoptosis and reduced invasiveness in glioblastoma,[19] and reduced cell proliferation, migration and tumor growth in breast cancer.[20] Recently, Medina et al. showed that overexpression of miR-21 leads to a pre-B malignant lymphoid-like phenotype and that inhibiting miR-21 alone induces complete tumor regression in a few days, demonstrating that miR-21 is a central oncomiR in tumor formation.[21]

miR-21 is clearly an important miRNA and there are emerging data on the role of miR-21 in many malignancies, including MM. In this study, we show that miR-21 inhibition causes increased apoptosis, reduced growth and an arrested cell cycle in human MM U266 cells. To further understand its molecular mechanism in the pathogenesis of MM, we carried out global proteomic profiling to identify targets of miR-21 in U266 cells. Using SILAC-based quantitative mass spectrometry we found that the expression of 178 out of 1498 proteins investigated was up-regulated by miR-21 inhibition. The predicted miR-21 targets (based on three different algorithms: miRBase,[22] TargetScan[23] and PicTar[24]) were highly enriched among the 178 up-regulated proteins. Using luciferase assays, we demonstrated that PIAS3 and PCBP1 identified from the proteomic screen are direct targets of miR-21 and that PIAS3 contributes to various phenotypic effects observed after miR-21 inhibition.

EXPERIMENTAL PROCEDURES

Cell Culture and Transfection

The human myeloma cell line U266 was purchased from American Type Culture Collections (Rockville, MD). U266 cells were cultured in RPMI 1640 supplemented with 1% penicillin/streptomycin, 1 mmol/L L-glutamine, and 10% fetal bovine serum at 37 °C, 5% CO_2 in air. For miR-21 inhibition, Locked nucleic acid (LNA)-modified anti-miR-21 oligonucleotides (designated as LNA-21) and negative control oligos (designated as LNA-cont) were purchased from Exiqon (Vedbaek, Denmark). For miR-21 enhancement, a miRIDIAN microRNA Mimic for miR-21 (designated as MIM-21) and a negative control (designated as MIM-cont) were purchased from Dharmacon (Chicago, IL). Transfection with 100 nM MIM-21/MIM-cont or LNA-21/LNA-cont was performed using Nucleofector X005 (Amaxa, Cologne, Germany), according to an optimized protocol for the U266B1 cell line (http://www.lonzabio.com/fileadmin/groups/marketing/Downloads/Protocols/Generated/Optimized_Protocol_121.pdf). miRNA expression was verified after 72 h by quantitative real-time PCR (qRT-PCR) as described below.

RNA Extraction and qRT-PCR

Total RNA was extracted from cultured cells using Trizol Reagent (Invitrogen) according to the manufacturer's protocol. Reverse transcription was performed according to the protocol of the Improm-II Reverse Transcriptase System (Promega). qPCR was performed as described in the SYBR premix Ex Taq instructions (TaKaRa, Dalian, China) with an ABI Prism 7000 System (Applied Biosystems, Foster City, CA). GAPDH mRNA levels were used for normalization. For detection of miRNAs, miRNA was first isolated with an Ambion mirVana miRNA isolation kit (Ambion). A Nanodrop 2000 spectrophotometer (Thermo Scientific, Wilmington, DE) was used to detect the concentration of total miRNA. Quantitative analysis of miR-21 expression was assayed using a Hairpin-it miRNA real-time PCR Quantitation Kit (GenePharma, Shanghai, China). Each sample was analyzed in triplicate. U6 snRNA was used for normalization. The oligonucleotides used as primers were: miR-21-RT: 5′-GTCGTATCCAGTGCAGGGTCCGA GGTATTCGCACTGGATACGACTCAACA-3′, miR-21-F: 5′-GCCGCTAGCTTATCAGACTGATGT-3′, miR-21-R: 5′-GTGCAGGGTCCGAGGT-3′; U6-RT: 5′-GTCGTATCCAGTG CAGGGTCCGAGGTATTCGCACTGGATACGACAAAAATATG-3′, U6−F: 5′-GCGCGT CGTGAAGCGTTC-3′, U6-R: 5′-GTGCAGGGTCCGAGGT-3′; PIAS3-F: 5′-GCCGACATGGACGTGTCCTGTG-3′, PIAS3-R: 5′-TTCCCTCCTGGACTGCGCTGTAC-3′; CUL2-F: 5′-GTTCGTATCATGAAAGCACGAAAA-3′, CUL2-R: 5′-TTAAACCTAGCTCTTGACTG GCTAATC-3′; PCBP1-F: 5′-CAGAGGTGAAAGGCTATTGG-3′, PCBP1-R: 5′-GGCAGCA GAGCCAGTGATAG-3′; GAPDH-F: 5′-CCACCCATGGCAAATTCCATGGCA-3′, GAPDH -R: 5′-TCTAGACGGCAGGTCAGGTCCACC-3′; and CAPN2-F: 5′-GATTCATCCAGAAC GTGTAGG-3′, CAPN2-R: 5′-GGTTAAACACTGGAGCGTGTC-3′.

Cell Growth Assay

A Cell Counting Kit-8 (Dojindo Laboratories, Japan) was used to determine the viability of cells. In brief, cells were plated in 96-well plates at a density of one thousand cells per well. The cell proliferation reagent WST-8 (10 μL) was added to each well and cells were incubated for 3 h at 37 °C. Viable cell numbers were estimated by measuring the optical density (OD) at 450 nm. Absorbance of untreated U266 cells was set as 100% viability, and absorbance of cell-free wells containing medium was set as zero.

Detection of Apoptosis

Apoptosis was detected using Annexin V/PI (propidium iodide) staining. In brief, cells (1×10^6) were washed once in phosphate-buffered saline (PBS) and then stained with Annexin V-FITC and PI (2 mg/mL) (Biovision). Samples were acquired on a FACScan flow cytometer (Becton Dickinson, San Jose, CA) and analyzed with the WinMDI 2.8 software program.

Cell Cycle Analysis

Cells were harvested, washed with ice-cold PBS, fixed with 70% ethanol for 1 h at 4 °C, and pretreated with RNase (Worthington, Lakewood, NJ) for 30 min at 37 °C. Cells were stained with PI (Sigma Chemicals, St. Louis, MO), and a cell cycle profile was determined using a FACScan flow cytometer (Becton Dickinson). For each sample, 20000 events were acquired, and cell cycle distributions were determined using cell cycle analysis software (Modfit). Experiments were performed in triplicate. Results are presented as the percentage of cells in a particular phase.

SILAC Labeling

U266 cells were grown in SILAC RPMI 1640 Medium (Pierce Biotechnology, Rockford, IL) containing 10% v/v dialyzed FBS, and either 0.1 mg/mL heavy [$^{13}C_6$] or light [$^{12}C_6$] L-lysine (Pierce Biotechnology). Cells were propagated in SILAC medium for more than six generations to ensure nearly 100%

incorporation of labeled amino acids. "Heavy" labeled cells were transfected with 100 nM LNA-21 using a Nucleofector X005 (Amaxa, Cologne, Germany), according to an optimized protocol for the U266B1 cell line. "Light" labeled U266 cells were transfected with 100 nM negative control LNA-cont. After 72 h, cells were washed three times with ice-cold washing buffer (10 μM Tris−HCl, 250 μM sucrose, pH 7.0), transferred to a clean 1.5 mL eppendorf tube and lysed with RIPA lysis buffer (50 mM Tris-HCl, 150 mM NaCl, 0.1% SDS, 1% NP-40, 0.5% sodium deoxycholate, 1 mM PMSF, 100 mM leupeptin, and 2 mg/mL aprotinin, pH 8.0). Cellular debris was removed by centrifugation for 30 min at 13200× g, 4 °C. Protein concentrations were measured in duplicate using the RC DC protein assay (BioRad, Hercules, CA) and confirmed by SDS-PAGE.

Protein Separation and In-gel Digestion

The "light" and "heavy" lysates were mixed in a 1:1 ratio based on protein weight (50 μg of each), boiled in SDS-PAGE sample buffer, separated by 10% SDS-PAGE and stained with Coomassie Brilliant Blue (CBB). The entire gel lane was cut into 50 sections for in-gel tryptic digestion. Excised sections were chopped into small pieces, washed in water and completely destained using 100 mM ammonium bicarbonate in 50% ACN. A reduction step was performed by adding 100 μL 10 mM DTT at 37 °C for 3 h. Proteins were alkylated by adding 100 μL 50 mM iodoacetamide, and then were left in the dark at 20 °C to react for 30 min. The small gel pieces were first washed in water, then acetonitrile, and finally dried by SpeedVac for 30 min. Digestion was carried out using 20 μg/mL sequencing grade modified trypsin (Promega, Madison, WI) in 50 mM ammonium bicarbonate. Sufficient trypsin solution was added to swell the gel pieces, which were kept at 4 °C for 45 min and then incubated at 37 °C overnight. The gels were extracted once with extraction buffer (67% acetonitrile containing 2.5% trifluoroacetic acid). The peptide extract and the supernatant of the gel slice were combined and then completely dried in a SpeedVac centrifuge.

Protein Identification and Quantification

The dried peptides from each gel slice were reconstituted in 5% ACN/0.1% formic acid and analyzed with an Ultimate3000 nano HPLC system (Dionex, Sunnyvale, CA) coupled to an LTQ Orbitrap mass spectrometer (Thermo Fisher Scientific) via a nanoelectrospray ion source (Proxeon Biosystems). Peptide mixtures from each gel slice were loaded at a flow rate of 30 μL/min in 95% buffer C (2% acetonitrile, 0.1% trifluoroacetic acid in HPLC grade water) and 5% buffer B (98% acetonitrile, 0.1% formic acid in HPLC grade water) onto a PepMap100 trapping column (0.3 mm × 5 mm). After 5 min, peptides were eluted and separated on an LC Packings PepMap C18 column (3 μm, 0.075 × 150 mm) by a linear gradient from 5% to 40% of buffer B in buffer A (2% acetonitrile and 0.1% formic acid) at a flow rate of 300 nL/min over 120 min. The remaining peptides were eluted by a gradient from 40 to 100% buffer B over 5 min. The general mass spectrometric parameters were as follows: spray voltage, 1.8 kV; capillary voltage, 4 V; ion transfer tube temperature, 200 °C; tube lens voltage, 100 V. Data-dependent acquisition was performed on LTQ-Orbitrap using Xcalibur 2.07 software (Thermo Fisher Scientific). Full scan MS spectra (m/z 300 to 2000; resolution of 60000 at m/z 400) were acquired with the Orbitrap. Automatic gain control (AGC) was set to 5×10^5 ions and a maximum fill time of 750 ms. After a brief survey scan, the six most intense multiply charged ions were selected for fragmentation by low energy collision-induced dissociation (CID) in the linear ion trap, simultaneous with the completion of the MS scan in the Orbitrap. The AGC of the LTQ was set to 10000 ions and a maximum fill time of 150 ms. Fragmentation was carried out at a normalized collision energy of 35% with an activation q = 0.25 and an activation time of 30 ms. The ion selection threshold was set to 5000. Fragmentation of previously selected precursor ions was dynamically excluded for the following 45 s. The raw MS/MS data were searched using TurboSEQUEST (ThermoElectron, San Jose, CA) against a real and against a reverse IPI Human 3.47 database (each database including 72082 protein entries) to identify peptides. The following search criteria were employed: full tryptic specificity was required; two missed cleavages were allowed; parent ion mass tolerance 20 ppm; fragment ion tolerance 0.5 Da; Cys (+57.0215 Da, Carbamidomethylation) was set as a fixed modification, whereas Met (+15.9949 Da, Oxidation), and Lys (+6.0201 Da, SILAC heavy amino acid) were considered as variable modifications. SEQUEST criteria were Xcorr ≥1.9 for $[M + H]^{1+}$ ions, ≥ 2.4 for $[M + 2H]^{2+}$ ions, and ≥3.5 for $[M + 3H]^{3+}$ ions, and ΔCn ≥ 0.1 for the identification of fully tryptic peptides. Using this combination of filters, the protein false discovery rate was less than 1%. If peptide charge and peptide sequence in the same group were the same, we selected the peptide with the highest Xcorr value. Proteins matching at least two reliable unique peptides were considered as positively identified proteins. All identified peptides were subjected to relative quantification analysis using the program Census.[25] This program quantifies relative abundances of light and heavy versions of precursor peptides identified by MS^2 spectra. Only proteins with a minimum of two quantifiable peptides were included in our final data set. The protein ratios were calculated from the average of all quantified peptides.

Bioinformatic Analysis

Predicted miR-21 targets were identified using the algorithms of miRBase,[22] TargetScan[23] and PicTar.[24] Lists of predicted targets from each prediction program were compared to lists of up-regulated proteins. Enrichment of predicted targets was calculated by comparing the proportion of predicted targets among the up-regulated proteins to predicted targets among all proteins identified in the SILAC experiments.

mir-21-regulated proteins were classified based on the PANTHER (protein analysis through evolutionary relationships) system (http://www.pantherdb.org), a unique resource that classifies genes and proteins by their functions.[26] Some proteins were annotated manually based on literature searches and closely related homologues.

To determine if a given type of protein was overrepresented, enrichment analysis of Gene Ontology (GO) terms[27] and Kyoto Encyclopedia of Genes and Genomes (KEGG) pathways[28] was performed using DAVID (Database for Annotation, Visualization and Integrated Discovery) 6.7 (http://david.abcc.ncifcrf.gov/).[29,30] The default human proteome was used as the background list. The significance of enrichments was statistically evaluated with a modified Fisher's exact test (EASE score), and a p-value for each term was calculated by applying a Benjamini-Hochberg false discovery rate correction.[29,30] For GO term enrichments, the GO fat annotation available in DAVID was used. GO fat is a subset of the GO term set created by filtering out the broadest ontology terms to not overlook

more specific ones. The enrichment of GO biological process terms was also analyzed using Cytoscape and its Plugin, the Biological Networks Gene Ontology tool (BiNGO) 2.3,[31] using the complete GO term set and a hypergeometric statistical test with Benjamini-Hochberg false discovery rate correction. The GO slim generic assignment, the distribution of cellular components, molecular functions and biological processes of the mir-21 regulated proteins were analyzed (Table 1).

Table 1. GO Terms Enriched in miR-21-Regulated Proteins[a]

GO term	description	count[b]	%[c]	*P*-value[d]
GO:0006412	Translation	17	9.82	3.48×10^{-7}
GO:0000723	Telomere maintenance	7	4.04	3.59×10^{-7}
GO:0032200	Telomere organization	7	4.04	4.49×10^{-7}
GO:0006417	Regulation of translation	10	5.78	1.30×10^{-5}
GO:0046907	Intracellular transport	21	12.13	1.53×10^{-5}
GO:0000166	Nucleotide binding	61	35.26	1.04×10^{-12}
GO:0003723	RNA binding	31	17.91	$1.03 \times 10^{-1}0$
GO:0032553	Ribonucleotide binding	51	29.47	1.15×10^{-10}
GO:0032555	Purine ribonucleotide binding	51	29.47	1.15×10^{-10}
GO:0017076	Purine nucleotide binding	52	30.05	1.64×10^{-10}
GO:0005829	Cytosol	39	22.54	3.97×10^{-9}
GO:0043232	Intracellular nonmembrane-bounded organelle	54	31.21	1.73×10^{-7}
GO:0043228	Nonmembrane-bounded organelle	54	31.21	1.73×10^{-7}
GO:0070013	Intracellular organelle lumen	40	23.12	2.82×10^{-6}
GO:0043233	Organelle lumen	40	23.12	4.95×10^{-6}

[a]Top 5 GO biological process, molecular function and cellular component terms enriched in the miR-21-regulated proteins are listed. A complete list can be found in Table S3−S5, Supporting Information. [b]Number of miR-21-regulated proteins. [c]Percentage of mapped proteins associated with each term. [d]Statistical significance of the difference between the fraction of miR-21-regulated proteins assigned to this GO term and the fraction of all proteins within the human protein set assigned to this GO term.

Western Blotting

Protein extracts (30 μg) prepared with RIPA lysis buffer (50 mM Tris-HCl, 150 mM NaCl, 0.1% SDS, 1% NP-40, 0.5% sodium deoxycholate, 1 mM PMSF, 100 mM leupeptin, and 2 mg/mL aprotinin, pH 8.0) were resolved on a 10% SDS-PAGE gel, and transferred to an Immobilon-P PVDF transfer membrane (Millipore, Bedford, MA) by electroblotting. After blocking with 5% nonfat milk, membranes were probed with rabbit anti-CUL2 polyclonal, mouse anti-CAPN2 monoclonal (Santa Cruz Biotechnology, Santa Cruz, CA), mouse anti-PIAS3 monoclonal, rabbit anti-PCBP1 polyclonal, rabbit anti-ACTIN polyclonal (Abcam, Cambridge, MA), rabbit anti-STAT3-pY705 polyclonal, and rabbit anti-STAT3 polyclonal antibodies (Cell Signaling, Danvers, MA). Blots were then incubated with peroxidase-conjugated antimouse or antirabbit IgG (KPL, Gaithersburg, MD) for 1 h at room temperature at a 1:1000 dilution and then developed using a SuperSignal West Pico kit (Pierce Biotechnology, Rockford, IL). Immunoblots were scanned using an Image Scanner (GE healthcare, Uppsala, Sweden). Blot densitometry analysis was performed using ImageJ (National Institutes of Health).

Luciferase Assays

For reporter gene assays, the 3′-UTR fragments of CUL2, CAPN2, PCBP1 and PIAS3 were PCR-amplified from U266 total cDNA and cloned into a pGL3-control vector (Promega, Madison, WI) at the *Bgl*II restriction site and designated as pGL3-CUL2-WT, pGL3-CAPN2-WT, pGL3-PCBP1-WT and pGL3-PIAS3-WT, respectively. Mutated plasmids pGL3-PIAS3-Mut (the UAAGCU sequence in the complementary site for the seed region of miR-21 was mutated to UCCUAU), pGL3-PCBP1-Mut (AUAAGCU to AGCCUAU), pGL3-CAPN2-Mut (UAAGCU to UCCUAU) and pGL3-CUL2-Mut (GAUAAC to GCGCCC) were generated from pGL3-PIAS3-WT, pGL3-PCBP1-WT, pGL3-CAPN2-WT and pGL3-CUL2-WT, respectively, using a QuikChange kit (Stratagene, La Jolla, CA). Mutations are underlined. All pGL3 constructs were confirmed by DNA sequence analysis. pGL3 constructs and the Renilla luciferase plasmid phRL-SV40 (Promega) were cotransfected with 100 nM LNA-21 oligo or control LNA-cont oligo using a Nucleofector X005 (Amaxa). 48 h after transfection, luciferase assays were performed using a dual luciferase reporter assay system (Promega). Firefly luciferase activity was normalized to Renilla luciferase activity for each transfected well. Values from LNA-21 oligos were normalized to control LNA-cont oligos. *P*-values were calculated using two-tailed *t*-tests to compare relative luciferase activities for each construct.

siRNA Transfection

For PIAS3 gene silencing, an siRNA duplex (designated as si-PIAS3) targeted against PIAS3 (sense, 5′-GGAGCCAAAUGU-GAUUAUAUU-3′; antisense, 5′-UAUAAUC ACAUUUGG-CUCCUU-3′) and a negative control (designated as si-cont) siRNA duplex (sense, 5′-UUCUCCGAACGUGUCACGUTT-3′; antisense, 5′-ACGUGACAC GUUCGGAGAATT-3′) were purchased from Shanghai GenePharma Co. (Shanghai, China). Transfection with 100 nM si-PIAS3 or si-cont was performed usinga Nucleofector X005 (Amaxa) as described above. Cells were collected 72 h later and PIAS3 gene knockdown was assessed by Western blotting. STAT3 gene silencing was achieved by transfecting U266 cells with pSiStrike/STAT3 or pSiStrike/control vectors as described earlier.[32] Plasmid transfection was performed using a Nucleofector X005 (Amaxa). The resulting STAT3 knockdown and control cell lines were designated as U266-KD and U266-NC, respectively. Stat3 gene knockdown was assessed by Western blotting. Cell viability and apoptosis were assessed as described above.

Plasmid Constructs and Transient Transfection

The human PIAS3 expression plasmid (pPIAS3) (Catalog No.: EX-P0028-M77) and blank plasmid (pVector) were purchased from GeneCopoeia, Inc. (Germantown, MD). The PIAS3 and control plasmids were expressed in U266 cells by transient transfection using Nucleofector X005 as described above. Cells were collected 72 h later and overexpression of PIAS3 was confirmed by Western blotting. Cell viability and apoptosis were assessed as described above.

Confocal Fluorescence Microscopy

U266 cells were transfected with the LNA-21/cont oligo or MIM-21/cont as described above and grown on poly-L-lysine-treated glass coverslips. Cells were fixed 72 h after culture with 4% paraformaldehyde and permeabilized by 0.1% Triton X-100. After washing briefly in PBS, slides were blocked with 1% BSA for 1 h and then incubated with rabbit anti-STAT3 or anti-

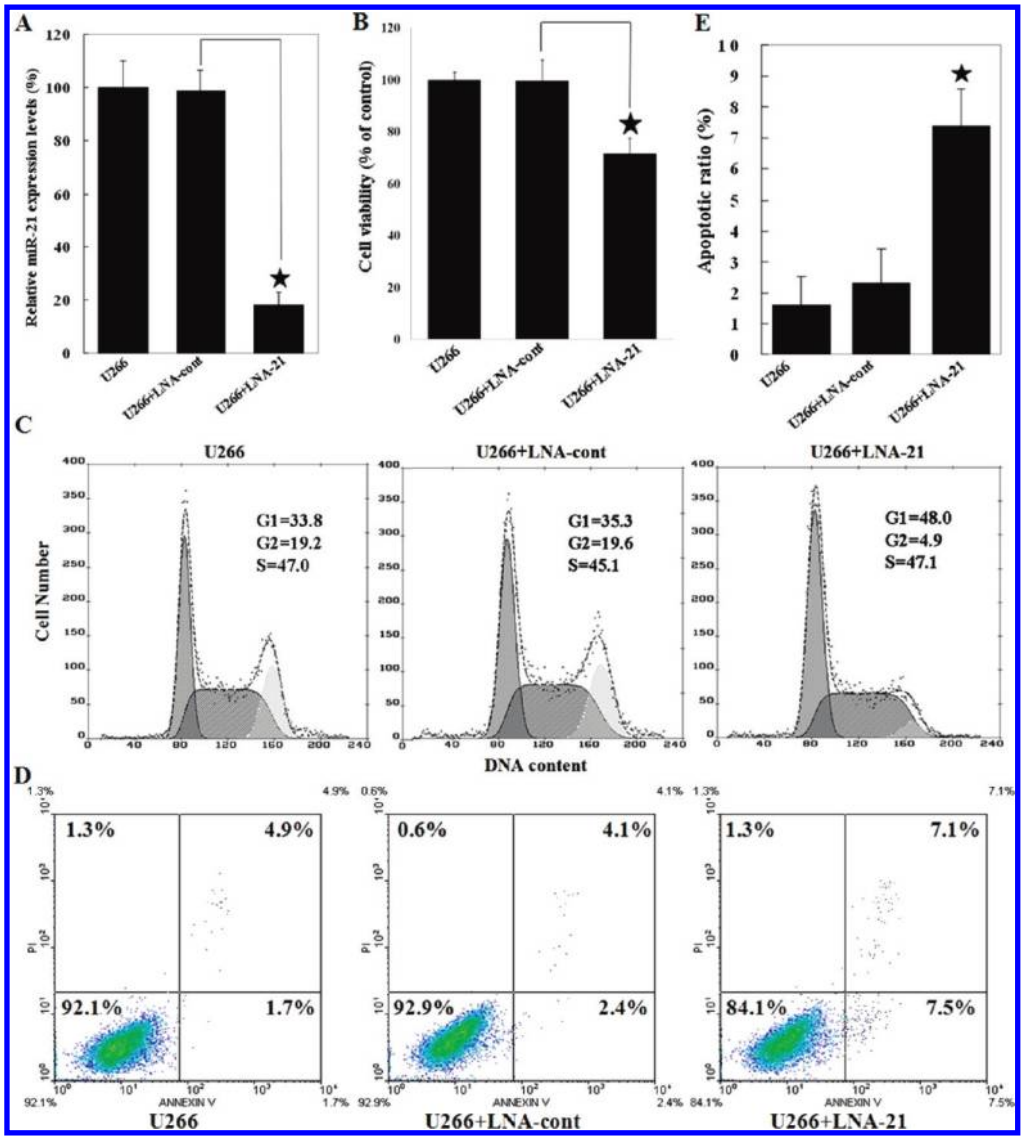

Figure 1. Effects of miR-21 inhibition on U266 cells. (A) miR-21 expression levels were significantly inhibited by more than 80% in LNA-21 transfected U266 cells relative to LNA-cont transfected cells. Relative miR-21 expression levels were examined by qRT-PCR (mean ± S.D., $*p < 0.01$). U6 snRNA was used as an internal standard. (B) Cell growth assays showed that miR-21 inhibition led to slower growth in U266 cells (mean ± S.D., $*p < 0.05$). (C) Flow cytometry showed that miR-21 inhibition produced a G1-phase arrest in U266 cells. (D) miR-21 inhibition resulted in a marked increase in the number of apoptotic cells. *X*-axis, AnnexinV; *Y*-axis, PI staining. Cell percentages are quantified in each quadrant. (E) Quantification of apoptosis induced by miR-21 inhibition in U266 cells as determined by flow cytometry. Data are expressed as means ± SD of apoptotic cells from at least three experiments, $*p < 0.05$.

STAT3-pY705 polyclonal and mouse anti-PIAS3 monoclonal antibodies at a dilution of 1:400. Cells were then washed three times with PBS and incubated with Cy5-conjugated goat antirabbit and rhodamine-conjugated goat antimouse IgGs (Pierce Biotechnology) at a dilution of 1:200 for 1 h. After washing and mounting, cells were examined using a LSM 510 laser scanning confocal microscope (Carl Zeiss, Jena, Germany). Images were taken with a 63× oil immersion objective lense at identical settings.

STAT3 Luciferase Reporter Assay

STAT3 luciferase reporter assay was performed essentially as described earlier.[33] In brief, U266 cells were transfected with the LNA-21 and/or pPIAS3 plasmids, a Stat3 firefly luciferase reporter plasmid pStat3-TA-luc (Clontech, Mountain View, CA) and a control Renilla luciferase reporter plasmid pRL-TK (Clontech) using a Nucleofector X005 (Amaxa). Luciferase activity was determined 48 h after transfection using a Dual-Luciferase Reporter Assay kit (Promega, Madison, WI) according to the manufacturer's protocol. Experiments were performed in triplicate. Luciferase values were normalized by transfection efficiency as measured by β-galactosidase. All data represent mean values ± s.d. of three independent experiments.

RESULTS

Effects of miR-21 Inhibition on U266 Cell Growth, Cell Cycle and Apoptosis

miR-21 is overexpressed in many human cancers and has been reported to be associated with multiple cancer-related processes including proliferation, apoptosis, invasion, and metastasis. In addition, other studies have shown that miR-21 is overexpressed in multiple myeloma cells.[4] To address the biological function of miR-21 in U266 cells, we used LNA-21 to

dx.doi.org/10.1021/pr201079y | J. Proteome Res. 2012, 11, 2078−2090

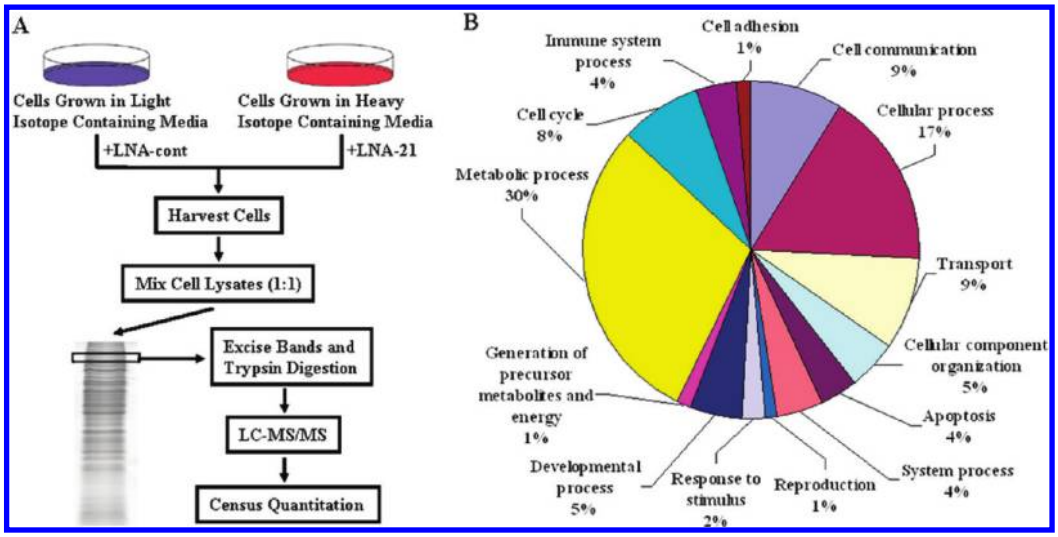

Figure 2. Quantitative proteomic identification of miR-21 targets in U266 cells. (A) Workflow for the identification of miR-21 targets. U266 cells were differentially labeled by growing them in medium containing light or heavy amino acids (SILAC). After transfection with anti-miR-21 locked nucleic acid (LNA-21) or control LNA (LNA-cont), cells were lysed, combined, and analyzed by quantitative proteomics. (B) Pie chart representations of the distribution of identified miR-21 regulated proteins according to their biological processes. Categorizations were based on information provided by the online resource PANTHER classification system.

downregulate miR-21. Optimal doses and time points for transfection of LNA reagents were determined by evaluating miR-21 levels using qRT-PCR (data not shown). As shown in Figure 1A, transfection of LNA-21 reduced miR-21 levels more than 80% in U266 cells, compared with cells transfected with negative control LNA-cont or untreated cells. MiR-21 inhibition significantly suppressed cell growth (Figure 1B) compared to untreated cells and those transfected with negative control LNA-cont. After 72 h, 48.0% of LNA-transfected U266 cells were in the G1 cell phase, 4.9% in G2 and 47.1% were in the S phase. Cells in G1 phase were significantly increased ($p < 0.05$). This demonstrates that miR-21 inhibition produced a G1-phase arrest in U266 cells (Figure 1C). We next examined whether miR-21 inhibition induced apoptosis in U266 cells using flow cytometry. Flow cytometry demonstrated that transfection of U266 cells with LNA-21 for 72 h resulted in a significant increase in the percentage of apoptotic cells, compared with cells transfected with negative control or untreated cells (Figure 1D). Quantitative analysis indicated that the percentage of apoptotic cells in LNA-21-transfected cells (7.4 ± 1.2%) was significantly higher ($p < 0.05$; Figure 1E) than that of the negative control-transfected group (2.3 ± 1.1%). These data demonstrate the tumorigenic properties of miR-21 in regulating cell growth, the cell cycle and apoptosis in myeloma cells.

Identification of miR-21 Targets using a Quantitative Proteomic Approach

Since miR-21 is expressed at high levels in the myeloma cell line U266, we reasoned that downregulation of miR-21 would increase the expression of its targets. To identify potential miR-21 target genes, we used quantitative proteomics and SILAC to identify proteins differentially expressed in U266 cells with or without miR-21 overexpression. Figure 2A shows the workflow in this quantitative proteomic approach. According to the criteria described in the Experimental Procedures, a total of 1498 nonredundant proteins were quantified (Table S1, Supporting Information). In line with common approaches for SILAC analyses,[34,35] we set the threshold for up- or down-regulated proteins at 2.0-fold. We found 178 up-regulated and 25 down-regulated proteins in U266 cells 72 h following transfection of LNA-21 (Table S2, Supporting Information). This overall increase in the levels of regulated proteins is consistent with the concept of microRNA-mediated translational inhibition.

To understand the biological relevance of miR-21 regulated proteins, the PANTHER classification system was used to categorize these proteins according to their biological processes. miR-21 regulated proteins were classified into 14 groups according to biological processes (Figure 2B). The largest group is involved in metabolic processes (29%). Significant numbers of miR-21-regulated proteins were also implicated in cellular processes (17%), cell communication (9%), the cell cycle (8%), and apoptosis (4%), indicating that miR-21 regulates diverse cellular functions involving widespread biological processes. It should be stated that many of these proteins are multifunctional and are assigned to more than one functional class. For example, the cell cycle and apoptosis classes contain 30 and 14 proteins, respectively (Table S3, Supporting Information). Of these, six proteins, including CUL2, EIF4G2, FKBP5, PRKDC, PTK2, and UBE2O, are involved in the regulation of both the cell cycle and apoptosis. This may partly explain why miR-21 inhibition resulted in an arrested cell cycle and in increased apoptosis.

Next, we tested how miRNA target predictions correlate with our data. miR-21 target predictions were obtained with three different algorithms: miRBase,[22] TargetScan[23] and PicTar.[24] As shown in Figure S1A (Supporting Information), predicted targets for miR-21 were highly enriched among the up-regulated proteins, compared to all the proteins identified in our SILAC experiments. Comparison of our data set with two previous proteomic studies revealed significant overlap but also differences (Figure S1B). Of the 178 upregulated proteins reported in this study, 15 (8.4%) and 25 (13.5%) were also reported as potential targets of miR-21 by Schramedei et al.[36] and Yang et al.,[37] respectively (Figure S1B). It is worth mentioning that 15 out of 16 potential targets of miR-21 reported by Schramedei et al.[36] were also identified in our

dx.doi.org/10.1021/pr201079y | J. Proteome Res. 2012, 11, 2078–2090

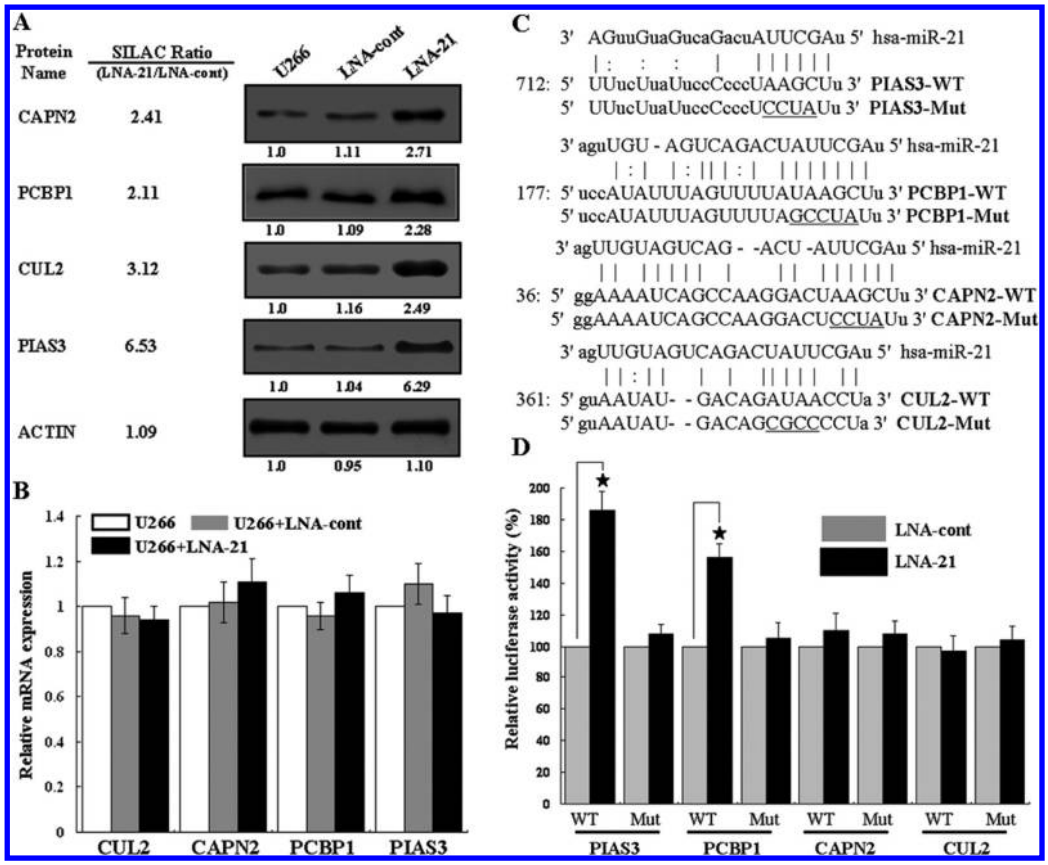

Figure 3. Validation of candidate miR-21 target genes. (A) Western blot showing LNA-21-mediated upregulation of CUL2, CAPN2, PCBP1 and PIAS3. U266 cells were transfected with LNA-21 or negative control LNA-cont, and incubated for 72 h. Thereafter, cell lysates were analyzed by Western blotting. Equal loading was confirmed by probing the same filters with actin. Numbers indicate quantification relative to the corresponding actin loading control and were determined using ImageJ. (B) U266 cells were transfected with LNA-21 or negative control LNA-cont and incubated for 72 h. Thereafter, total cellular RNAwas isolated and analyzed by qRT-PCR for the expression of CUL2, CAPN2, PCBP1 and PIAS3 mRNAs. Results, normalized for GAPDH, are shown as relative expression using the negative control miRNA as a reference. Data were collected from three independent experiments, which were run with three replicates (mean ± S.D.). (C) Putative miR-21-binding sites within the 3′-UTRs of CUL2, CAPN2, PCBP1 and PIAS3 genes. Perfect matches are indicated by a line, and G:U pairs by a colon. Nucleotides mutated for the reporter gene assays are underlined. (D) Activity of luciferase reporters containing wild type (WT) or mutated (Mut) putative miR-21 target sites in the 3′-UTRs of CUL2, CAPN2, PCBP1 and PIAS3. The relative luciferase activities normalized to corresponding transfections with LNA-cont oligos are shown. Data are shown as the mean ± SD of three replicates and are representative of three independent experiments. *$p < 0.05$.

experiment, indicating the reliability of our results (Figure S1B). One of the most frequently validated miR-21 targets, PDCD4, was among the upregulated proteins (Table S2, Supporting Information), further supporting the reliability of our data. Differences between our results and those reported by others may be due to differences in cell lines, cell culture conditions, quantitative methods, or mass spectrometry platforms used. The limited overlap between our SILAC and Yang et al.'s iTRAQ results is not unexpected, as previous studies have shown that SILAC and iTRAQ both possess distinct strengths and weaknesses and provide complementary types of information.[38] Therefore, the current proteomic study based on the SILAC method represents a complementary strategy for identifying miR-21 target genes.

GO and Signaling Pathway Analysis of miR-21 Target Proteins

To gain insights into the functional roles of miR-21, the overrepresentation (enrichment) of ontology terms and components of molecular pathways among miR-21 regulated proteins was compared with their occurrence in the human proteome. First, a GO slim generic assignment gave us an overview of the GO distribution (Figure S2, Supporting Information). Next, we performed GO biological process, molecular function and cellular component analyses (Tables S4−S6, Supporting Information). GO biological process analysis provided a comprehensive picture of miR-21 regulated proteins; translation, telomere maintenance and organization, intracellular transport, mRNA metabolic processes, post transcriptional regulation of gene expression, cytoskeleton organization, and RNA processing categories were all overrepresented. Since miR-21 acts as a negative regulator of gene expression by binding to the 3′-untranslated region (UTR) of its target mRNA, a large number of proteins (17; GO term: 0006396) which were annotated as involved in RNA processing (p-value = 1.84×10^{-4}) were identified in our study. The biological process terms were visualized as a network diagram where direct links describe the hierarchy and relationships between terms (Figure S3, Supporting Information). The colored nodes are those determined to be significantly overrepresented. By looking at the closest branch points of the overrepresented GO biological processes, we found six main functional groups that were strongly enriched in miR-21 regulated proteins, including three clusters of metabolic processes and three clusters of cellular processes (Figure S3). In the GO molecular functions

dx.doi.org/10.1021/pr201079y | J. Proteome Res. 2012, 11, 2078−2090

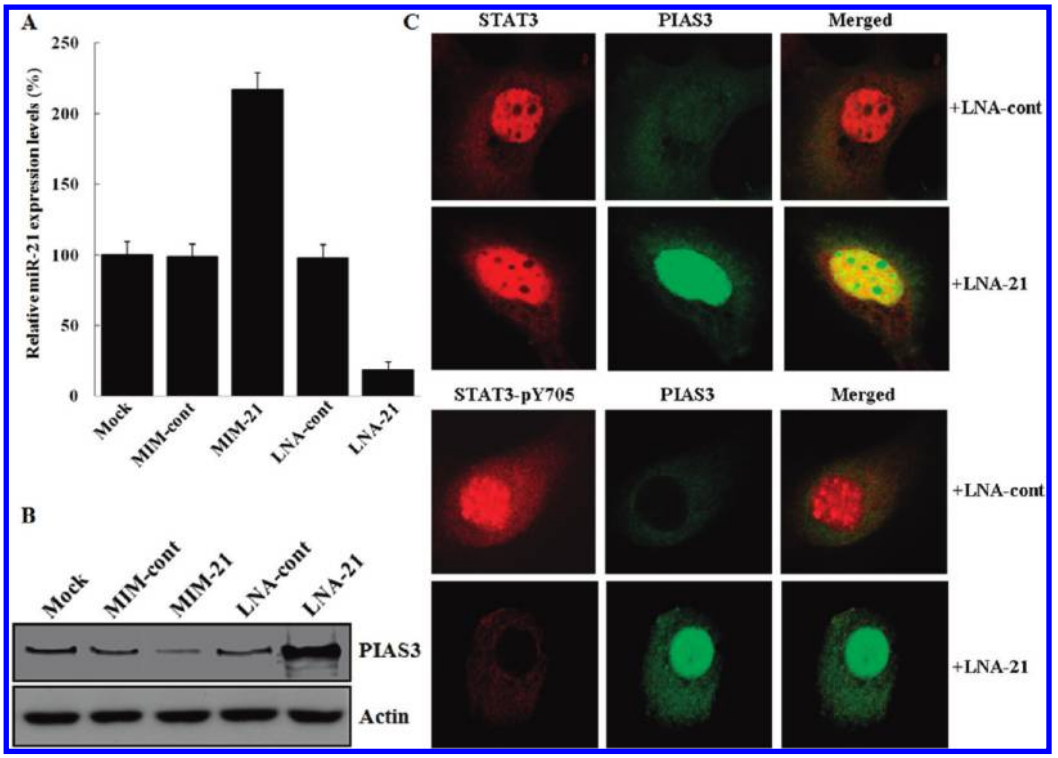

Figure 4. miR-21 negatively regulates PIAS3 protein expression in U266 cells. (A) qRT-PCR of miR-21 in U266 cells following transfection with LNA-21 or LNA-cont or with MIM-21 or MIM-cont. (B) U266 cell lysates were prepared and Western blotting of PIAS3 was performed 72 h post transfection. Overexpression and knock down of miR-21 had opposite effect on PIAS3 protein expression in U266 cells. (C) miR-21 inhibition increased the expression of PIAS3 and decreased STAT3 phosphorylation. The protein levels of PIAS3, total and phosphorylated STAT3 were monitored using confocal laser scanning.

category, we found that the most overrepresented functions were involved in nucleic acid binding, and included nucleotide binding, RNA binding, ribonucleotide binding, purine ribonucleotide binding, and purine nucleotide binding (Table S5, Supporting Information). In addition, functions including ATP binding, protein C-terminus binding, GTP binding, cytoskeletal protein binding, and structure-specific DNA binding were also significantly overrepresented ($p < 0.01$). In the GO cellular component category, we found that most of the miR-21 regulated proteins were enriched in nonmembrane-bound organelles (p-value $=1.73 \times 10^{-7}$), the cytosol (p-value $=3.97 \times 10^{-9}$) and organelle lumens (p-value $= 4.95 \times 10^{-6}$) (Table S6, Supporting Information). In addition, 22 miR-21 regulated proteins were attributed to the mitochondrion (p-value $=0.004$).

To reveal pathways in which miR-21 regulated proteins might be involved, we performed a search against the human KEGG pathways database (http://www.genome.jp/kegg/tool/color_pathway.html). As shown in Table S7 (Supporting Information, miR-21 regulated proteins are involved in pathways responsible for the control of key physiological and pathological processes. In particular, the pathways listed in Table S7 highlight the role of miR-21 regulated proteins in key mechanisms implicated in RNA processing. Of these, 11 proteins were mapped to RNA transport and 8 to the spliceosome. The deregulation of these pathways can lead to the establishment of pathological conditions such as cancer (e.g., "renal cell carcinoma") and neurodegenerative disorders (e.g., "Huntington's disease"). Interestingly, we found 3 miR-21 regulated proteins, CRKL, PAK2 and PTK2, which take part in the ErbB signaling pathway (Table S7), a pathway which couples the binding of extracellular growth factor ligands to intracellular signaling pathways regulating diverse biological responses, including proliferation, differentiation, cell motility, and survival. These results may imply a direct involvement of miR-21 in complex physiological and pathological systems, such as cell proliferation, differentiation, motility, cancers and neurodegenerative disorders.

Validation of Candidate miR-21 Target Genes

We selected four candidates of biological interest (CUL2, CAPN2, PCBP1 and PIAS3) from among the 178 genes up-regulated by LNA-21 transfection for further validation. CUL2, CAPN2 and PCBP1 were chosen for their role in inducing apoptosis. In addition, PIAS3 was selected as it showed the strongest up-regulation (6.3-fold; Table S2, Supporting Information) and is involved in myeloma pathogenesis.[39]

First, differential regulation of these candidate target genes by miR-21 in U266 cells was validated at the protein level by Western blotting. As shown in Figure 3A, increased expression of all these genes at the protein level was induced by miR-21 inhibition and their pattern of expression was the same as that obtained from SILAC experiments.

Second, we used qRT-PCR to examine changes in mRNA abundance for these candidate target genes. As shown in Figure 3B, none of the genes showed significantly increased mRNA expression as a result of miR-21 inhibition. Our results suggest that it is likely that these four targets are regulated by miR-21 mainly through translational inhibition instead of mRNA degradation.

Third, we performed luciferase assays to determine if miR-21 regulates these candidate targets directly. The 3′-UTR seed sequences of these candidate targets were predicted using the

dx.doi.org/10.1021/pr201079y | J. Proteome Res. 2012, 11, 2078–2090

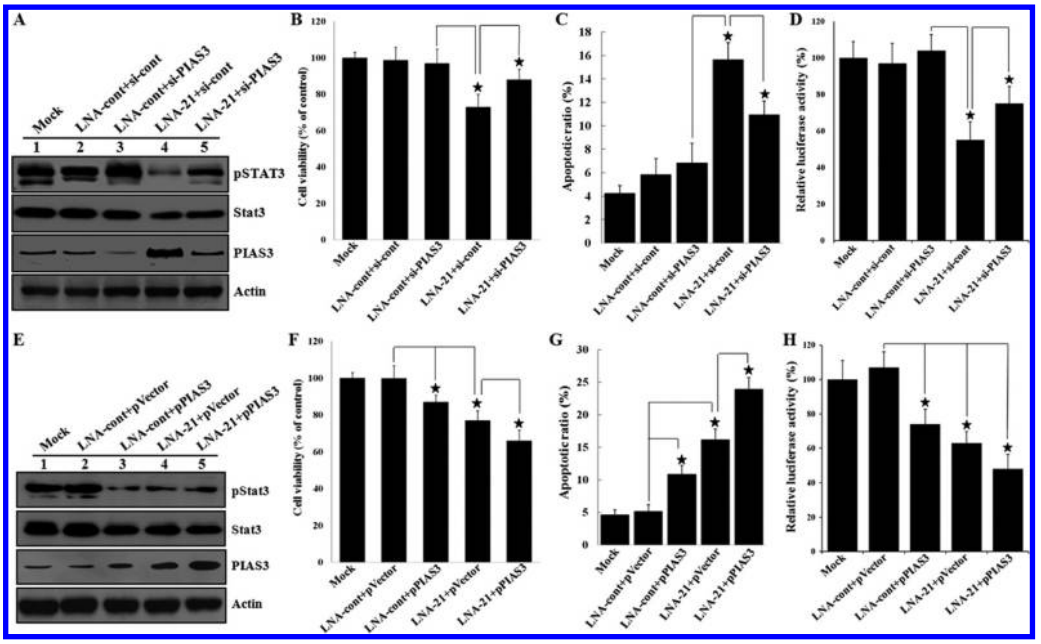

Figure 5. PIAS3 contributes to the oncogenic potential of miR-21 and STAT3 activity in U266 cells. (A) miR-21 knockdown inhibits constitutively active STAT3 in U266 cells and silencing of PIAS3 in LNA-21 treated cells and reverses the effect of miR-21 inhibition on STAT3 phosphorylation. U266 cells transfected with LNA-21 and/or PIAS3-specific small-interfering RNA (siRNA) and their corresponding controls for 72 h. Cell lysates were analyzed for protein levels of PIAS3, and total and phosphorylated STAT3, as indicated. Cell growth, apoptosis and luciferase reporter gene assays further revealed that silencing PIAS3 partially abrogated LNA-21-induced (B) cell growth, (C) apoptosis and (D) Stat3-mediated transcriptional activity. LNA-21, the PIAS3-expressing plasmid and their corresponding controls were introduced into U266 cells, as indicated, and (E) protein levels of PIAS3, and total and phosphorylated STAT3, (F) cell growth, (G) apoptosis and (H) Stat3-mediated transcriptional activity were assayed.

algorithms of miRanda[40,41] (Figure 3C) and then cloned downstream of the luciferase ORF. The constructs were cotransfected with LNA-21 or control LNA-cont into U266 cells. As shown in Figure 3D, significantly increased luciferase activity was observed in pGL3-PIAS3-WT or pGL3-PCBP1-WT transfected cells upon miR-21 inhibition. In contrast, there was no significant change in luciferase activity in cells transfected with pGL3-CAPN2-WT or pGL3-CUL2-WT. Furthermore, miR-21 did not affect the luciferase activity of these four genes when their 3′-UTR sequences were mutated at the site complementary to the seed region of miR-21 (Figure 3D). Taken together, our results indicate that PIAS3 and PCBP1 are direct targets of miR-21 in U266 cells, while CAPN2 and CUL2 are regulated by miR-21 indirectly.

Silencing of PIAS3 Reverses the Effect of miR-21 Inhibition on Activated STAT3, Cell Growth and Apoptosis

The role of the newly identified miR-21 target, PIAS3, on the growth and/or apoptosis of U266 cells was evaluated, after silencing and overexpression of PIAS3 by transient transfection of validated siRNAs and cDNAs. First, we studied the miR-21-mediated negative regulation of PIAS3 expression in U266 cells by Western blotting. We used an miR-21 mimic (MIM-21) or LNA-21 to enhance or reduce cellular miR-21 levels, respectively. Reduction or enhancement of miR-21 levels was confirmed by qRT-PCR (Figure 4A). PIAS3 protein levels were examined by Western blotting. As shown in Figure 4B, overexpression and knockdown of miR-21 had opposite effect on PIAS3 protein expression in U266 cells. Since previous studies have shown that STAT3 activation is downregulated by miR-21 knockdown[42,43] and increasing concentrations of PIAS3 result in a proportional decrease in STAT3 phosphorylation,[44] the interactions between miR-21, PIAS3 and STAT3 were examined in LNA-21 or LNA-cont transfected U266 cells using confocal laser scanning. As shown in Figure 4C, no significant change was noted in total STAT3 expression in U266 cells transfected with LNA-21 or control oligos. In contrast, compared with cells transfected with control oligos, miR-21 inhibition significantly increased expression of PIAS3 and decreased STAT3 phosphorylation (Figure 4C). Interestingly, PIAS3 and STAT3 were colocalized in the nucleus of cells that were transfected with LNA-21 (Figure 4C). These results indicate that miR-21 negatively regulates PIAS3 protein expression in U266 cells.

To further explore if silencing PIAS3 reverses the effect of LNA-21 on STAT3 activation, cell viability, apoptosis and transcriptional activity, U266 cells were cotransfected with LNA-21 and siRNA against PIAS3 to inhibit miR-21 and PIAS3 expression, respectively. As shown in Figure 5A lane 4, transfection of LNA-21 resulted in the up-regulation of PIAS3 expression in U266 cells compared to LNA-cont-transfected cells (lane 2), while siRNA against PIAS3 inhibited PIAS3 expression in LNA-21-transfected (lane 5) and LNA-cont transfected cells (lane 3) compared to control siRNA-transfected cells (lane 2). No significant change was noted in STAT3-pTyr705 and total STAT3 expression in U266 cells transfected with PIAS3 siRNA (lane 3) or control oligos (lane 2). In contrast, a decrease in STAT3-pTyr705 was observed in LNA-21-transfected cells (lane 4) and an increase in STAT3-pTyr705 was seen in cells cotransfected with PIAS3 and LNA-21 siRNA (lane 5). Furthermore, cotransfection of U266 cells with siRNA of PIAS3 and LNA-21 partially abrogated LNA-21-induced cell growth inhibition and apoptosis (Figures 5B and C). We further measured the effects of miR-21 on STAT3 activity using luciferase reporter gene assays. As shown in

dx.doi.org/10.1021/pr201079y | J. Proteome Res. 2012, 11, 2078−2090

Figure 5D, knockdown of miR-21 in U266 cells yielded a significant decrease in STAT3-dependent relative luciferase activity, while cotransfection of U266 cells with PIAS3 siRNA and LNA-21 markedly enhanced Stat3-mediated transcriptional activity in U266 cells. Overexpression experiments conducted by transfection of cDNAs corresponding to the coding sequences of PIAS3 gave similar results. PIAS3 overexpression resulted in decreased STAT3 phosphorylation, cell viability, increased apoptosis and transcriptional activity (Figure 5E–H). To investigate whether STAT3 plays a role in cell growth and apoptosis, we used RNAi to reduce cellular STAT3 levels. A stable U266 cell line was established by expressing shRNA that targets STAT3 mRNA, termed U266-KD. Western blotting demonstrated a reduction in the expression level of STAT3 and phospho-STAT3 (pY705) proteins in this cell line (Figure S4A, Supporting Information). We next studied the consequences of STAT3 inhibition, as shown in Figure S4B; suppression of STAT3 led to a significant decrease in the proliferation of U266 cells compared with control cells. This decrease in STAT3 also led to an increased rate of apoptosis (Figure S4C). Based on these data, we propose that miR-21 functions as a negative regulator of PIAS3 and that at least some of the various biological effects of miR-21 are mediated by regulation of PIAS3 expression in myeloma cells.

With regards to PCBP1, silencing or overexpression of PCBP1 did not affect the growth and apoptosis of U266 cells in basal conditions or after treatment with LNA-21 (data not shown).

DISCUSSION

miR-21 is overexpressed in multiple types of cancer, including breast, pancreatic, colorectal, and multiple myeloma[16] and has emerged as a key regulator of oncogenic processes.[45] Considerable attention has thus been given to determining its functions as well as to identifying its target genes. Here, since miR-21 is upregulated in MM cells, we performed a loss-of-function study by knocking down miR-21 in MM cells. The function of miR-21 in U266 cells was examined by depleting mature miR-21 using LNA oligonucleotides complementary to miR-21. We found that knocking down miR-21 induces apoptosis and inhibits cell growth in myeloma cells (Figure 1), suggesting that miR-21 plays an important role in MM tumorigenesis.

It is well-known that miRNAs regulate biological processes by suppressing the expression of their target proteins.[46] To understand the mechanism underlying the potential role of miR-21 in MM, it is essential to first identify its target proteins. Previous studies have shown that one miRNA can modulate the levels of hundreds of proteins.[7] High-throughput methods are thus required for miRNA target identification. In the present study, we performed quantitative SILAC experiments together with bioinformatic predictions, and functional assays to identify miR-21 protein targets in MM cells. Using this approach, we identified 178 proteins that are up-regulated by miR-21 knockdown.

Of all the miR-21 regulated proteins, PIAS3 (protein inhibitor of activated STAT3) showed the strongest up-regulation (6.3-fold; Table S2, Supporting Information) following miR-21 inhibition in our study. Western blotting and luciferase assays further confirmed it as a direct target. PIAS3 was originally identified as a specific inhibitor of the STAT3 signaling pathway and plays an important role as a direct negative regulator of STAT3 activity.[47] Recent data have shown that PIAS3 and STAT3 function as transcriptional coregulators to modulate the activity of a diverse set of transcription factors, including NF-κB,[48] a zinc finger protein Gfi-1,[49] microphthalmia transcription factor,[50] nuclear receptor coactivator TIF2,[51] and Smads.[52] The mechanisms involved in the binding of PIAS3 to its targets and its modulation of their transcription are being explored. For example, PIAS3 was found to suppress NF-κB -mediated transcription by interacting with its p65/RelA subunit[48] and to inhibit gene induction through activated STAT3 by blocking its DNA binding activity.[53] It is of particular interest that PIAS3 has been shown to inhibit the IL-6-triggered STAT3 signaling pathway in MM cells,[39] since constitutive activation of STAT3 signaling has long been associated with MM cells.[54] Furthermore, loss of PIAS3 expression at the protein but not the mRNA level has been shown to occur in glioblastoma multiforme when STAT3 phosphorylation and activity increases.[55] Recently, Dabir et al. demonstrated that increasing concentrations of PIAS3 result in a proportional decrease in STAT3 phosphorylation and transcription activity.[44] Their results suggest that PIAS3 may inhibit STAT3 by accelerating the dephosphorylation process.[44] Consistent with these reports, our results show that PIAS3 overexpression results in decreased STAT3 phosphorylation and transcription activity (Figure 5), suggesting that PIAS3 may play a role in the dephosphorylation process of STAT3 in myeloma cells. However, the precise role of PIAS3 in the regulation of STAT3 phosphorylation and transcription activity in MM cells remains unclear.

A growing body of evidence has shown that miR-21 is involved in the regulation of STAT3 signaling pathways.[15,42] Recently, miR-21 was reported to upregulate STAT3 expression in a positive feedback loop.[43] miR-21 is overexpressed in all types of human cancers.[16] Interestingly, constitutively activated STAT3 has been reported in all of these cancers,[15] underscoring the pivotal role of miR-21 in the oncogenic potential of STAT3 and its involvement in the pathogenesis of MM and other cancers.

It is thus highly interesting that we found that miR-21 functions as a negative regulator of PIAS3 and that at least some of the various biological effects of miR-21 are mediated by the regulation of PIAS3 expression in U266 cells. By investigating the impact of STAT3 inhibition and PIAS3 knockdown/overexpression in U266 cells, we have shown that the apoptosis and cell growth inhibition induced by miR-21 knockdown appear to be mediated in part by up-regulated PIAS3. In contrast to the knockdown of PIAS3 that reduces the effects of miR-21 inhibition on U266 cells, overexpression of PIAS3 enhances the effects of miR-21 inhibition on U266 cells. Since overexpression of PIAS3 alone can lead to the induction of apoptosis, development of inhibitors of miR-21 or activators of PIAS3 may find therapeutic applications on MM.

In our study, we also identified 25 proteins that are downregulated >2.0-fold due to the inhibition of miR-21 (Table S2, Supporting Information). These downregulated proteins may represent potential targets or may be due to the indirect effects of miR-21. Although miRNAs are generally known to down-regulate gene expression by inhibiting translation or inducing target mRNA degradation, a growing number of studies have demonstrated that miRNAs can also upregulate the expression of their targets under certain circumstances.[56,57] For example, miR-346 activates the activity of receptor-interacting protein 14 by increasing its protein expression[57] and miR-373 has been reported to target the

promoter sequences of E-cadherin and cold-shock domain-containing protein C2 to induce their expression.[58] Therefore, further experiments are required to determine whether any of these LNA-21-downregulated proteins are direct targets of miR-21.

In conclusion, we have demonstrated that SILAC is an efficient and reliable method for functionally identifying miRNA targets. Using this proteomic approach we identified proteins regulated by miR-21 in myeloma cells and showed by further experiments that PIAS3 is a direct target of miR-21. The cross talk between miR-21, PIAS3, and STAT3 are summarized schematically in Figure 6. In U266 cells, constitutively activated

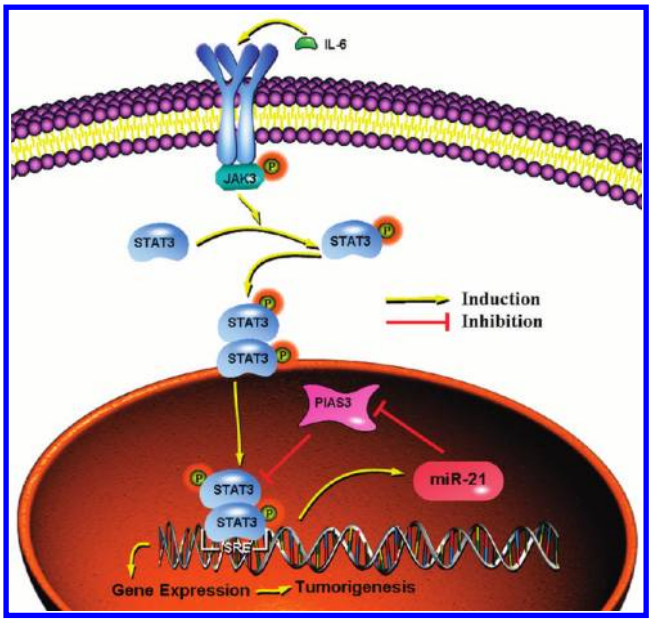

Figure 6. Putative model of the cross talk between miR-21, PIAS3 and STAT3 in U266 cells. STAT3 is activated by IL-6 or other cytokines through phosphorylation of the tyrosine residue of STAT3 by Janus Kinase (JAK) or other kinases. Phosphorylation of the tyrosine residue of STAT3 results in homodimerization of STAT3 and its translocation into the nucleus to function as a transcription factor. In the nucleus, activated STAT3 induces the overexpression of miR-21, and in a positive feedback loop, the overexpression of miR-21 directly targets PIAS3 and activates STAT3-dependent transcription through inhibition of PIAS3. ISRE stands for Interferon Stimulated Response Element.

Stat3 induces miR-21 overexpression, and in a positive feedback loop, miR-21 upregulates STAT3 activity by inhibiting PIAS3. MiR-21 targets PIAS3 directly, and PIAS3 is a negative regulator of STAT3 activation. The elucidation of the role of PIAS3 in the miR-21-Stat3 positive regulatory loop, therefore, may not only shed light into the molecular basis of the biological effects of miR-21 observed in MM cells, but also provides a direct target for the development of novel anti-MM therapeutic strategies. It is now important to further characterize the interactions between miR-21 and individual target proteins and to determine the full significance of gene regulation by miR-21 in MM cells.

■ ASSOCIATED CONTENT

Supporting Information

Supplemental figures and tables. This material is available free of charge via the Internet at http://pubs.acs.org.

■ AUTHOR INFORMATION

Corresponding Author

*Prof. Feng Ge, Institute of Hydrobiology, Chinese Academy of Sciences. E-mail: gefeng@ihb.ac.cn. Phone/Fax: +86-27-68780500. Prof. Li-Jun Bi, Institute of Biophysics, Chinese Academy of Sciences. E-mail: blj@sun5.ibp.ac.cn. Phone/Fax: +86-10-64871293.

Author Contributions

⊥These authors contributed equally to this work.

Notes

The authors declare no competing financial interest.

■ ACKNOWLEDGMENTS

This work was supported by the National Basic Research Program of China (973 Program, 2012CB518700), the Hundred Talents Program of the Chinese Academy of Sciences, and the Open Research Fund of the National Laboratory of Biomacromolecules.

■ ABBREVIATIONS

MM, multiple myeloma; SILAC, stable isotope labeling by amino acids in cell culture; STAT3, signal transducer and activator of transcription 3; PIAS3, protein inhibitor of activated STAT3; UTR, untranslated region; LNA, locked nucleic acid; PANTHER, protein analysis through evolutionary relationships

■ REFERENCES

(1) Raab, M. S.; Podar, K.; Breitkreutz, I.; Richardson, P. G.; Anderson, K. C. Multiple myeloma. *Lancet* **2009**, *374* (9686), 324−39.

(2) Ge, F.; Bi, L. J.; Tao, S. C.; Xu, X. D.; Zhang, Z. P.; Kitazato, K.; Zhang, X. E. Proteomic analysis of multiple myeloma: current status and future perspectives. *Proteomics Clin. Appl.* **2011**, *5* (1−2), 30−7.

(3) Caers, J.; Vande broek, I.; De Raeve, H.; Michaux, L.; Trullemans, F.; Schots, R.; Van Camp, B.; Vanderkerken, K. Multiple myeloma--an update on diagnosis and treatment. *Eur. J. Haematol.* **2008**, *81* (5), 329−43.

(4) Pichiorri, F.; Suh, S. S.; Ladetto, M.; Kuehl, M.; Palumbo, T.; Drandi, D.; Taccioli, C.; Zanesi, N.; Alder, H.; Hagan, J. P.; Munker, R.; Volinia, S.; Boccadoro, M.; Garzon, R.; Palumbo, A.; Aqeilan, R. I.; Croce, C. M. MicroRNAs regulate critical genes associated with multiple myeloma pathogenesis. *Proc. Natl. Acad. Sci. U.S.A.* **2008**, *105* (35), 12885−90.

(5) Carthew, R. W.; Sontheimer, E. J. Origins and Mechanisms of miRNAs and siRNAs. *Cell* **2009**, *136* (4), 642−55.

(6) Brodersen, P.; Voinnet, O. Revisiting the principles of microRNA target recognition and mode of action. *Nat. Rev. Mol. Cell. Biol.* **2009**, *10* (2), 141−8.

(7) Baek, D.; Villen, J.; Shin, C.; Camargo, F. D.; Gygi, S. P.; Bartel, D. P. The impact of microRNAs on protein output. *Nature* **2008**, *455* (7209), 64−71.

(8) Iorio, M. V.; Croce, C. M. MicroRNAs in cancer: small molecules with a huge impact. *J. Clin. Oncol.* **2009**, *27* (34), 5848−56.

(9) Lu, J.; Getz, G.; Miska, E. A.; Alvarez-Saavedra, E.; Lamb, J.; Peck, D.; Sweet-Cordero, A.; Ebert, B. L.; Mak, R. H.; Ferrando, A. A.; Downing, J. R.; Jacks, T.; Horvitz, H. R.; Golub, T. R. MicroRNA expression profiles classify human cancers. *Nature* **2005**, *435* (7043), 834−8.

(10) Esquela-Kerscher, A.; Slack, F. J. Oncomirs - microRNAs with a role in cancer. *Nat. Rev. Cancer* **2006**, *6* (4), 259−69.

(11) Djuranovic, S.; Nahvi, A.; Green, R. A parsimonious model for gene regulation by miRNAs. *Science* **2011**, *331* (6017), 550−3.

(12) Pichiorri, F.; Suh, S. S.; Rocci, A.; De Luca, L.; Taccioli, C.; Santhanam, R.; Zhou, W.; Benson, D. M. Jr.; Hofmainster, C.; Alder,

H.; Garofalo, M.; Di Leva, G.; Volinia, S.; Lin, H. J.; Perrotti, D.; Kuehl, M.; Aqeilan, R. I.; Palumbo, A.; Croce, C. M. Downregulation of p53-inducible microRNAs 192, 194, and 215 impairs the p53/MDM2 autoregulatory loop in multiple myeloma development. *Cancer Cell* **2010**, *18* (4), 367−81.
(13) Zhou, Y.; Chen, L.; Barlogie, B.; Stephens, O.; Wu, X.; Williams, D. R.; Cartron, M. A.; van Rhee, F.; Nair, B.; Waheed, S.; Pineda-Roman, M.; Alsayed, Y.; Anaissie, E.; Shaughnessy, J. D. Jr. High-risk myeloma is associated with global elevation of miRNAs and overexpression of EIF2C2/AGO2. *Proc. Natl. Acad. Sci. U.S.A.* **2010**, *107* (17), 7904−9.
(14) Gutierrez, N. C.; Sarasquete, M. E.; Misiewicz-Krzeminska, I.; Delgado, M.; De Las Rivas, J.; Ticona, F. V.; Ferminan, E.; Martin-Jimenez, P.; Chillon, C.; Risueno, A.; Hernandez, J. M.; Garcia-Sanz, R.; Gonzalez, M.; San Miguel, J. F. Deregulation of microRNA expression in the different genetic subtypes of multiple myeloma and correlation with gene expression profiling. *Leukemia* **2010**, *24* (3), 629−37.
(15) Loffler, D.; Brocke-Heidrich, K.; Pfeifer, G.; Stocsits, C.; Hackermuller, J.; Kretzschmar, A. K.; Burger, R.; Gramatzki, M.; Blumert, C.; Bauer, K.; Cvijic, H.; Ullmann, A. K.; Stadler, P. F.; Horn, F. Interleukin-6 dependent survival of multiple myeloma cells involves the Stat3-mediated induction of microRNA-21 through a highly conserved enhancer. *Blood* **2007**, *110* (4), 1330−3.
(16) Krichevsky, A. M.; Gabriely, G. miR-21: a small multi-faceted RNA. *J. Cell. Mol. Med.* **2009**, *13* (1), 39−53.
(17) Folini, M.; Gandellini, P.; Longoni, N.; Profumo, V.; Callari, M.; Pennati, M.; Colecchia, M.; Supino, R.; Veneroni, S.; Salvioni, R.; Valdagni, R.; Daidone, M. G.; Zaffaroni, N. miR-21: an oncomir on strike in prostate cancer. *Mol. Cancer* **2010**, *9*, 12.
(18) Si, M. L.; Zhu, S.; Wu, H.; Lu, Z.; Wu, F.; Mo, Y. Y. miR-21-mediated tumor growth. *Oncogene* **2007**, *26* (19), 2799−803.
(19) Chan, J. A.; Krichevsky, A. M.; Kosik, K. S. MicroRNA-21 is an antiapoptotic factor in human glioblastoma cells. *Cancer Res.* **2005**, *65* (14), 6029−33.
(20) Yan, L. X.; Wu, Q. N.; Zhang, Y.; Li, Y. Y.; Liao, D. Z.; Hou, J. H.; Fu, J.; Zeng, M. S.; Yun, J. P.; Wu, Q. L.; Zeng, Y. X.; Shao, J. Y. Knockdown of miR-21 in human breast cancer cell lines inhibits proliferation, in vitro migration and in vivo tumor growth. *Breast Cancer Res.* **2011**, *13* (1), R2.
(21) Medina, P. P.; Nolde, M.; Slack, F. J. OncomiR addiction in an in vivo model of microRNA-21-induced pre-B-cell lymphoma. *Nature* **2010**, *467* (7311), 86−90.
(22) Griffiths-Jones, S.; Saini, H. K.; van Dongen, S.; Enright, A. J. miRBase: tools for microRNA genomics. *Nucleic Acids Res.* **2008**, *36* (Database issue), D154−8.
(23) Lewis, B. P.; Burge, C. B.; Bartel, D. P. Conserved seed pairing, often flanked by adenosines, indicates that thousands of human genes are microRNA targets. *Cell* **2005**, *120* (1), 15−20.
(24) Krek, A.; Grun, D.; Poy, M. N.; Wolf, R.; Rosenberg, L.; Epstein, E. J.; MacMenamin, P.; da Piedade, I.; Gunsalus, K. C.; Stoffel, M.; Rajewsky, N. Combinatorial microRNA target predictions. *Nat. Genet.* **2005**, *37* (5), 495−500.
(25) Park, S. K.; Venable, J. D.; Xu, T.; Yates, J. R. 3rd A quantitative analysis software tool for mass spectrometry-based proteomics. *Nat. Methods* **2008**, *5* (4), 319−22.
(26) Mi, H.; Guo, N.; Kejariwal, A.; Thomas, P. D. PANTHER version 6: protein sequence and function evolution data with expanded representation of biological pathways. *Nucleic Acids Res.* **2007**, *35* (Database issue), D247−52.
(27) Ashburner, M.; Ball, C. A.; Blake, J. A.; Botstein, D.; Butler, H.; Cherry, J. M.; Davis, A. P.; Dolinski, K.; Dwight, S. S.; Eppig, J. T.; Harris, M. A.; Hill, D. P.; Issel-Tarver, L.; Kasarskis, A.; Lewis, S.; Matese, J. C.; Richardson, J. E.; Ringwald, M.; Rubin, G. M.; Sherlock, G. Gene ontology: tool for the unification of biology. The Gene Ontology Consortium. *Nat. Genet.* **2000**, *25* (1), 25−9.
(28) Kanehisa, M.; Goto, S. KEGG: kyoto encyclopedia of genes and genomes. *Nucleic Acids Res.* **2000**, *28* (1), 27−30.
(29) Huang da, W.; Sherman, B. T.; Lempicki, R. A. Systematic and integrative analysis of large gene lists using DAVID bioinformatics resources. *Nat. Protoc.* **2009**, *4* (1), 44−57.
(30) Huang da, W.; Sherman, B. T.; Lempicki, R. A. Bioinformatics enrichment tools: paths toward the comprehensive functional analysis of large gene lists. *Nucleic Acids Res.* **2009**, *37* (1), 1−13.
(31) Maere, S.; Heymans, K.; Kuiper, M. BiNGO: a Cytoscape plugin to assess overrepresentation of gene ontology categories in biological networks. *Bioinformatics* **2005**, *21* (16), 3448−9.
(32) Ge, F.; Zhang, L.; Tao, S. C.; Kitazato, K.; Zhang, Z. P.; Zhang, X. E.; Bi, L. J. Quantitative proteomic analysis of tumor reversion in multiple myeloma cells. *J. Proteome Res.* **2011**, *10* (2), 845−55.
(33) Zhang, J.; Chen, F.; Li, W.; Xiong, Q.; Yang, M.; Zheng, P.; Li, C.; Pei, J.; Ge, F. 14-3-3ζ Interacts with Stat3 and Regulates Its Constitutive Activation in Multiple Myeloma Cells. *PLoS One* **2012**, *7* (1), e29554.
(34) Pan, C.; Olsen, J. V.; Daub, H.; Mann, M. Global effects of kinase inhibitors on signaling networks revealed by quantitative phosphoproteomics. *Mol. Cell. Proteomics* **2009**, *8* (12), 2796−808.
(35) Lam, Y. W.; Evans, V. C.; Heesom, K. J.; Lamond, A. I.; Matthews, D. A. Proteomics analysis of the nucleolus in adenovirus-infected cells. *Mol. Cell. Proteomics* **2010**, *9* (1), 117−30.
(36) Schramedei, K.; Morbt, N.; Pfeifer, G.; Lauter, J.; Rosolowski, M.; Tomm, J. M.; von Bergen, M.; Horn, F.; Brocke-Heidrich, K. MicroRNA-21 targets tumor suppressor genes ANP32A and SMARCA4. *Oncogene* **2011**, *30*, 2975−85.
(37) Yang, Y.; Chaerkady, R.; Beer, M. A.; Mendell, J. T.; Pandey, A. Identification of miR-21 targets in breast cancer cells using a quantitative proteomic approach. *Proteomics* **2009**, *9* (5), 1374−84.
(38) Shui, W.; Gilmore, S. A.; Sheu, L.; Liu, J.; Keasling, J. D.; Bertozzi, C. R. Quantitative proteomic profiling of host-pathogen interactions: the macrophage response to Mycobacterium tuberculosis lipids. *J. Proteome Res.* **2009**, *8* (1), 282−9.
(39) Wang, L. H.; Yang, X. Y.; Mihalic, K.; Xiao, W.; Li, D.; Farrar, W. L. Activation of estrogen receptor blocks interleukin-6-inducible cell growth of human multiple myeloma involving molecular cross-talk between estrogen receptor and STAT3 mediated by co-regulator PIAS3. *J. Biol. Chem.* **2001**, *276* (34), 31839−44.
(40) Enright, A. J.; John, B.; Gaul, U.; Tuschl, T.; Sander, C.; Marks, D. S. MicroRNA targets in Drosophila. *Genome Biol.* **2003**, *5* (1), R1.
(41) John, B.; Enright, A. J.; Aravin, A.; Tuschl, T.; Sander, C.; Marks, D. S. Human MicroRNA targets. *PLoS Biol.* **2004**, *2* (11), e363.
(42) Zhou, X.; Ren, Y.; Moore, L.; Mei, M.; You, Y.; Xu, P.; Wang, B.; Wang, G.; Jia, Z.; Pu, P.; Zhang, W.; Kang, C. Downregulation of miR-21 inhibits EGFR pathway and suppresses the growth of human glioblastoma cells independent of PTEN status. *Lab. Invest.* **2010**, *90* (2), 144−55.
(43) Yang, C. H.; Yue, J.; Fan, M.; Pfeffer, L. M. IFN induces miR-21 through a signal transducer and activator of transcription 3-dependent pathway as a suppressive negative feedback on IFN-induced apoptosis. *Cancer Res.* **2010**, *70* (20), 8108−16.
(44) Dabir, S.; Kluge, A.; Dowlati, A. The association and nuclear translocation of the PIAS3-STAT3 complex is ligand and time dependent. *Mol. Cancer Res.* **2009**, *7* (11), 1854−60.
(45) Selcuklu, S. D.; Donoghue, M. T.; Spillane, C. miR-21 as a key regulator of oncogenic processes. *Biochem. Soc. Trans.* **2009**, *37* (Pt 4), 918−25.
(46) Bartel, D. P. MicroRNAs: target recognition and regulatory functions. *Cell* **2009**, *136* (2), 215−33.
(47) Chung, C. D.; Liao, J.; Liu, B.; Rao, X.; Jay, P.; Berta, P.; Shuai, K. Specific inhibition of Stat3 signal transduction by PIAS3. *Science* **1997**, *278* (5344), 1803−5.
(48) Jang, H. D.; Yoon, K.; Shin, Y. J.; Kim, J.; Lee, S. Y. PIAS3 suppresses NF-kappaB-mediated transcription by interacting with the p65/RelA subunit. *J. Biol. Chem.* **2004**, *279* (23), 24873−80.
(49) Rodel, B.; Tavassoli, K.; Karsunky, H.; Schmidt, T.; Bachmann, M.; Schaper, F.; Heinrich, P.; Shuai, K.; Elsasser, H. P.; Moroy, T. The zinc finger protein Gfi-1 can enhance STAT3 signaling by interacting with the STAT3 inhibitor PIAS3. *EMBO J.* **2000**, *19* (21), 5845−55.

(50) Levy, C.; Nechushtan, H.; Razin, E. A new role for the STAT3 inhibitor, PIAS3: a repressor of microphthalmia transcription factor. *J. Biol. Chem.* **2002**, *277* (3), 1962−6.
(51) Jimenez-Lara, A. M.; Heine, M. J.; Gronemeyer, H. PIAS3 (protein inhibitor of activated STAT-3) modulates the transcriptional activation mediated by the nuclear receptor coactivator TIF2. *FEBS Lett.* **2002**, *526* (1−3), 142−6.
(52) Long, J.; Wang, G.; Matsuura, I.; He, D.; Liu, F. Activation of Smad transcriptional activity by protein inhibitor of activated STAT3 (PIAS3). *Proc. Natl. Acad. Sci. U.S.A.* **2004**, *101* (1), 99−104.
(53) Levy, C.; Lee, Y. N.; Nechushtan, H.; Schueler-Furman, O.; Sonnenblick, A.; Hacohen, S.; Razin, E. Identifying a common molecular mechanism for inhibition of MITF and STAT3 by PIAS3. *Blood* **2006**, *107* (7), 2839−45.
(54) Catlett-Falcone, R.; Landowski, T. H.; Oshiro, M. M.; Turkson, J.; Levitzki, A.; Savino, R.; Ciliberto, G.; Moscinski, L.; Fernandez-Luna, J. L.; Nunez, G.; Dalton, W. S.; Jove, R. Constitutive activation of Stat3 signaling confers resistance to apoptosis in human U266 myeloma cells. *Immunity* **1999**, *10* (1), 105−15.
(55) Brantley, E. C.; Nabors, L. B.; Gillespie, G. Y.; Choi, Y. H.; Palmer, C. A.; Harrison, K.; Roarty, K.; Benveniste, E. N. Loss of protein inhibitors of activated STAT-3 expression in glioblastoma multiforme tumors: implications for STAT-3 activation and gene expression. *Clin. Cancer Res.* **2008**, *14* (15), 4694−704.
(56) Henke, J. I.; Goergen, D.; Zheng, J.; Song, Y.; Schuttler, C. G.; Fehr, C.; Junemann, C.; Niepmann, M. microRNA-122 stimulates translation of hepatitis C virus RNA. *EMBO J.* **2008**, *27* (24), 3300−10.
(57) Tsai, N. P.; Lin, Y. L.; Wei, L. N. MicroRNA mir-346 targets the 5′-untranslated region of receptor-interacting protein 140 (RIP140) mRNA and up-regulates its protein expression. *Biochem. J.* **2009**, *424* (3), 411−8.
(58) Place, R. F.; Li, L. C.; Pookot, D.; Noonan, E. J.; Dahiya, R. MicroRNA-373 induces expression of genes with complementary promoter sequences. *Proc. Natl. Acad. Sci. U.S.A.* **2008**, *105* (5), 1608−13.